Finally, a brief summary of the energetics for various chemical processes involving the CCN diradicals is given in Figure 10 in which a schematic diagram contains different states for the NH + $C_2H_4$ system, CCN diradicals, and aziridine obtained from the dscribed CI, $T \rightarrow 0$ treatments. The relative energy levels for the same system have already been considered by Haines and Csizmadia.[6] It should be noted here that their singlet $CH_2CH_2NH$ correlated with the aziridine $S_1$ state seems to correspond to our zwitterionic state $^1FE_t^{zw}$ with a dominant contribution of $|a^2\rangle$ configuration. It is easy to depict from Figure 10 that the $^1FF$ diradical state correlates without doubt with the ground-state $S_0$ of aziridine.

One important facet which has totally been left out of consideration in this work is the problem concerning courses of isomerization for the CCN diradical other than the cyclization. This point, together with the overall kinetic phase of the $NH(^3\Sigma^-)$–ethylene reaction, will be reported elsewhere.

**Acknowledgment.** The authors are indebted to Professor R. J. Buenker for discussions and advice regarding the MRD-CI program. They are also grateful to Drs. K. Yamaguchi and H.-O. Beckmann for partial assistance in computations. It is a pleasure for one of the authors (T.F.) to express his particular appreciation of the Deutsche Forschungsgemeinschaft Richard-Merton visiting professorship, which enabled him to stay at the Freie Universität Berlin for the 1980–1981 winter during which most part of the present work was carried out. The computer times allocated by the Informatik-Rechnerbetrieb Technische Universität Berlin and by the Computer Center, Institute for Molecular Science, Okazaki, are also acknowledged.

**Registry No.** NH, 13774-92-0; $H_2$, 1333-74-0; $CH_2{=}CH_2$, 74-85-1; $\cdot CH_2CH_2NH\cdot$, 86239-28-3.

# Theoretical Investigation of the Elimination and Addition Reactions of Methane and Ethane with Nickel

**Margareta R. A. Blomberg, Ulf Brandemark, and Per E. M. Siegbahn***

*Contribution from the Institute of Theoretical Physics, University of Stockholm, S-11346 Stockholm, Sweden.* *Received March 4, 1983*

**Abstract:** Contracted CI calculations have been performed to study the mechanisms for the concerted elimination and addition reactions of ethane and methane with nickel. It is found that the $^1A_1$ state of nickel–ethane and the $^1A'$ state of nickel–methane behave very similarly. The elimination barrier, for example, is computed to be 34 kcal/mol for methane and 37 kcal/mol for ethane. For the addition reaction a somewhat larger difference is obtained, the activation energy of methane being 54 kcal/mol and of ethane (breaking the C–C bond) 42 kcal/mol. This difference in activation energy can be explained by the difference in the bond strength of the C–H bond in methane and the C–C bond in ethane, the C–H bond being 16 kcal/mol stronger. The difference between these two systems on one side and $H_2$ on the other is large; $H_2$ has a computed addition barrier to nickel of only 3 kcal/mol. The hydrogen atoms can much more easily form bonds in several directions at the same time than methyl groups, and this difference leads to higher activation energies for reactions involving methyl groups. For all three systems the reaction takes place with nickel in a $d^9$ state and with a large extent of d involvement in the bonding at the bent equilibrium geometry.

## 1. Introduction

In many catalytic processes involving transition metals the formation of new bonds occurs via reductive elimination reactions, and bonds are broken via oxidative addition reactions. The mechanisms for these two types of reactions, which are the reverse of each other, can be either concerted or nonconcerted. The nonconcerted reaction should in this case have a radical mechanism which would involve high activation energies. The purpose of the present study is therefore to investigate the concerted reaction mechanisms for different types of reactants. A homogeneous reductive elimination and oxidative addition reaction can be written:

$$L_nMR_1R_2 \rightleftarrows L_nM + R_1{-}R_2 \qquad (1)$$

where M is a transition metal, the L's are nonreacting ligands (type phosphines or carbonyls), and the reacting group $R_1$ and $R_2$ are hydrogen atoms or alkyl groups. From experiment it is well known that the ligands L can have a great influence on the reaction rate. The activation energy for elimination of butane from diethyl(dipyridyl)nickel is, for example, reduced from 66 to 16 kcal/mol upon complexation of an olefin.[1] The approach we have chosen is, however, to build up an understanding of these kinds of reactions from as simple models as possible, where we can study the electronic mechanisms of the bond-breaking and bond-forming processes in detail and then step by step investigate how different factors can influence the reaction. We have, therefore, not included any ligands L in this study in order to obtain accurate results for the pure elimination and addition reactions. The effects of different types of ligands are under investigation and will be presented in later papers.[2] Our specific purpose in this paper is to compare reaction mechanisms for the three classes of reactions represented by different combinations of R groups, H–H, H–alkyl, and alkyl–alkyl, and try to correlate these to experimental reaction rates. Methyl groups are used as models for alkyl groups and nickel for the transition metal. The results for H–H have been presented in previous papers on $NiH_2$[3] and will only be repeated here for the sake of comparison. In the present paper the details of the results for $Ni(H)CH_3$ and $Ni(CH_3)_2$ will be presented. In a forthcoming paper comparisons between nickel and palladium compounds will be presented together with the effects of introducing water ligands into the model.[4] Some of the results have been discussed earlier in ref 5.

(1) P. J. Davidson, M. F. Lappert, and R. Pearce, *Chem. Rev.*, **76**, 219 (1976); T. Yamamoto, A. Yamamoto, and S. Ikeda, *J. Am. Chem. Soc.*, **93**, 3350 (1971).

(2) U. Brandemark, M. R. A. Blomberg, and P. E. M. Siegbahn, to be submitted for publication.

(3) M. R. A. Blomberg and P. E. M. Siegbahn, *J. Chem. Phys.*, **78**, 986 (1983); *ibid.*, in press.

(4) U. Brandemark, M. R. A. Blomberg, L. G. M. Petterson, and P. E. M. Siegbahn, to be submitted for publication.

0002-7863/83/1505-5557$01.50/0 

There do not exist enough experimental data to give any definite order of the reaction rates for the three classes of reactants, H–H, H–alkyl, and alkyl–alkyl, and the data that do exist are somewhat ambiguous. In a theoretical paper by Balazs et al.[6] it is said that the rates of the reductive elimination reactions of the type represented by eq 1 appear to decrease in the order $k_{L_nMH_2} > k_{L_nM(H)CH_3} > k_{L_nM(CH_3)_2}$ for a series in which the metal and its ligands L are constant. In contradiction to this statement there exist experimental evidence that the elimination of H–alkyl is much faster than both the elimination of H–H and alkyl–alkyl.[7] The addition reaction is observed for H–H for several different metals, both homogeneously and heterogeneously, and recently evidence for the splitting of C–H bonds in addition reactions was obtained for iridium complexes.[8,9] Except for a couple of rather special cases there exists no example of a splitting of a C–C bond through an oxidative addition reaction. The formation of $Ni(CPh_3)_2$ from the triphenyl methyl dimer[10] has been reported as an example of this,[1] but it is doubtful whether the reaction mechanism really is a concerted oxidative addition. In any case the C–C bond to be broken in the triphenyl methyl dimer is an unusually weak one. The other case is the splitting of strained C–C bonds by metal atoms, e.g., the insertion of platinum into cyclopropane.[11] Also in this case the split C–C bond is unusually weak. It therefore seems as if the H–H bond is more easily broken in an oxidative addition reaction than the C–H and C–C bonds.

In order to investigate reaction rates and mechanisms for the above-mentioned systems, we have calculated the energies for reactions 1 and the electronic properties of the involved molecules. We have not determined complete reaction paths but only calculated the most interesting parts of the potential surfaces, i.e., minima and saddle points, thus determining barrier heights and equilibrium geometries. The calculations include correlation effects through the contracted CI method[12] with molecular orbitals obtained from CASSCF (complete active space SCF)[13] or SCF calculations. For certain parts of the potential surfaces, energy gradients are used at the SCF level.[14]

In the previous calculations on $NiH_2$[3] it was found that the $^1A_1$ state behaves differently during reaction 1 than the rest of the states investigated. This state has a bent equilibrium geometry with nickel in a $d^9$ s configuration. The d orbitals are strongly involved in the bonding and the binding energy is 8 kcal/mol. The barrier for reaching this equilibrium from $Ni(^1D)$ and $H_2$ is very small, only a few kilocalories/mole. The present investigation of the reactions of nickel with methane and ethane is therefore mainly concerned with the totally symmetric singlet states. To compare with $NiH_2$, the saddle point for the $^3B_1$ state, which is representative for the low triplet states of $NiH_2$, was also determined for $Ni(CH_3)_2$.

The relevance of the present study of reactions of ligand free nickel to real chemistry might be questioned. However, calculations on the same type of reactions with water ligands added to nickel are in progress.[2] The preliminary results show that the energetics of the reactions are affected by the ligands, but the character of the wave function remains. Nickel is dominated by a $d^9$ configuration also in the $(H_2O)_2NiR_2$ and $(H_2O)_2Ni$ complexes, and the nickel $d_{xz}$ orbital (see Figure 1 for the orientation of the coordinate system) is strongly involved in the Ni–R bonding.

In section 2 the details of the calculations are presented, and in section 3 the results for $Ni(CH_3)_2$ and $Ni(H)CH_3$ are reported. The conclusions of this study are summarized in section 4.

Comparisons will also be made with the following previous theoretical studies. Åkermark et al.[15] did SCF and valence CI calculations on several states of linear and bent $Ni(CH_3)_2$. Tatsumi et al.[16] did extended Hückel calculations on reductive elimination from nickel and palladium complexes. Balazs et al.[6] did $X\alpha$ calculations on a series of complexes as a basis for a discussion of reaction 1.

## 2. Computational Details

The basis set used for nickel is the same as in ref 3, which is the SDZC set (1) of Tatewaki et al.[17] with the following modifications. The 3d and 4s shells were split into two functions each, and two diffuse p functions (with exponents 0.112 and 0.0355) were added together with one diffuse d function (with exponent 0.1641). The basis for the active hydrogen (not belonging to a methyl group) was also taken from ref 3 and is the 5s basis of Huzinaga[18] contracted to 3s and augmented with one p function (0.8). For carbon the MIDI-3 basis for Tatewaki et al.[19] was used, and for the nonactive hydrogens (belonging to a methyl group) the 4s basis of Huzinaga[18] contacted to DZ. For the active hydrogen the same basis set as for $NiH_2$[3] was used, while for the rest of the hydrogens a smaller basis set was consequently used in order to make the calculations too large. This choice of basis set leads to an unequal treatment of the C–H bonds in methane at the asymptote, but as can be seen from Figure 3, the electron distribution in methane is only somewhat distorted, the charge on the active hydrogen being +0.07 and on each of the rest of the hydrogens +0.11. Since the basis sets for nickel and carbon are only of minimal basis quality for the core orbitals, the 1s, 2s, and 2p orbitals for nickel and the 1s orbital for carbon are kept frozen in their atomic shapes to avoid superposition errors.

For $NiH_2$ it was found that the wave function around the bent minimum was dominated by a single closed-shell configuration with a coefficient close to 0.9. It was therefore decided to optimize all the equilibrium geometry parameters in $Ni(CH_3)_2$ and $Ni(H)CH_3$ at the SCF level using energy gradients.[14] The so-obtained geometries of the $CH_3$ groups were then kept fixed in the determinations of the local minima and saddle points. The $R_1$–Ni–$R_2$ angle and the Ni–R distances for the equilibrium geometry were determined at the CI level using SCF or CASSCF orbitals. The saddle points were also determined at the CI level, by varying the same geometric parameters and the rocking angle $\alpha$ (see Figure 1). In this case CASSCF orbitals were used as one particle basis. At the dissociation limit, CASSCF plus CI calculations were performed for Ni plus ethane and methane, respectively, in their experimental geometries. For linear $Ni(CH_3)_2$ the geometry of the $CH_3$ groups was taken from ref 15. The Ni–C distance was optimized at the CI level using CASSCF orbitals. The saddle point for the $^3B_1$ state was determined in the same way as for the same state of $NiH_2$,[3] using combinations of two sets of SCF orbitals for the CI calculations.

In the CASSCF method[13] the occupied orbitals are divided into two sets: the inactive orbitals, which are doubly occupied in all configurations, and the active orbitals, in which the rest of the electrons are distributed in all possible ways. In the present calculations the active space was kept as small as possible, including only bonding and antibonding orbitals and those d orbitals which are not doubly occupied in the dominant configurations. For the linear and dissociated systems this principle leads to trivial choices of active spaces, determined by the atomic states of nickel. For the bent minima and saddle points the first choice had six

(5) M. Blomberg, U. Brandemark, L. Pettersson, and P. Siegbahn, *Int. J. Quantum Chem.*, **23**, 855 (1983).
(6) A. C. Balazs, K. H. Johnson, and G. M. Whitesides, *Inorg. Chem.*, **21**, 2162 (1982).
(7) J. R. Norton, *Acc. Chem. Res.*, **12**, 139 (1979).
(8) R. H. Crabtree, M. F. Mella, J. M. Mihelcic, and J. M. Quirk, *J. Am. Chem. Soc.*, **104**, 107 (1982).
(9) A. H. Janowicz and R. G. Bergman, *J. Am. Chem. Soc.*, **104**, 352 (1982).
(10) G. Wilke and H. Schott, *Angew. Chem.*, **78**, 592 (1966).
(11) D. J. Yarrow, J. A. Ibers, M. Lenarda, and M. Graziani, *J. Organomet. Chem.*, **70**, 133 (1974); J. Rajaram and J. A. Ibers, *J. Am. Chem. Soc.*, **100**, 829 (1978).
(12) P. E. M. Siegbahn, in "Current Aspects of Quantum Chemistry: Proceedings of the International Congress, Barcelona, Spain, 28 Sept–3 Oct 1981", R. Carbo, Ed., Elsevier, Amsterdam, 1981.
(13) P. E. M. Siegbahn, J. Almlöf, A. Heiberg, and B. O. Roos, *J. Chem. Phys.*, **74**, 2384 (1981).
(14) S. Saebö and J. Almlöf, the MOLECULE gradient program, Oslo, 1979.
(15) B. Åkermark, H. Johansen, B. Roos, and U. Wahlgren, *J. Am. Chem. Soc.* **101**, 5876 (1979).
(16) K. Tatsumi, R. Hoffmann, A. Yamamoto, and J. K. Stille, *Bull. Chem. Soc. Jpn.*, **54**, 1857 (1981).
(17) H. Tatewaki and S. Huzinaga, *J. Chem. Phys.*, **71**, 4339 (1979).
(18) S. Huzinaga, *J. Chem. Phys.*, **42**, 1293 (1965).
(19) H. Tatewaki and S. Huzinaga, *J. Comput. Chem.*, **1**, 205 (1980).

Table I. $Ni(CH_3)_2$ ($^1A_1$): Geometries[a] and Energies[b]

| geometry | R(Ni-C) | R(C-C) | θ | α | R(Ni-CC) | rel energy[c] |
|---|---|---|---|---|---|---|
| asymptote ($Ni(^1D) + C_2H_6$) | | 2.92 | | | 15.0 | 0 |
| transition state | 4.03 | 3.91 | 58 | 35 | 3.53 | 42.3 |
| bent equilibrium | 3.93 | 5.77 | 94.3 | −11.5 | 2.67 | 5.3 |
| linear equilibrium | 3.89 | 7.78 | 180 | 0 | 0 | 23.8 |

[a] Distances in atomic units and angles in degrees. For definition of the angles see Figure 1. [b] Energies in kilocalories/mole. [c] Computed splitting between the $^1D(d^9s)$ and $^3F(d^8s^2)$ states of nickel is 14.8 kcal/mol. The experimental value is 7.0 kcal/mol.[21]

Table II. $Ni(H)CH_3$ ($^1A'$): Geometries[a] and Energies[b]

| geometry | R(Ni-C) | R(Ni-H) | R(C-H) | θ | α | R(Ni-CH) | rel energy |
|---|---|---|---|---|---|---|---|
| asymptote ($Ni(^1D) + CH_4$) | | | 2.07 | | | 100.0 | 0 |
| transition state | 4.00 | 2.80 | 3.07 | 50 | 25 | 3.08 | 54.1 |
| equilibrium | 3.74 | 2.78 | 4.81 | 94.0 | 2 | 2.22 | 20.7 |

[a] Distances in au and angles in deg. For definition of the angles see Figure 1. [b] Energies in kcal/mol.

active electrons in five active orbitals, including the two bonds and two antibonding orbitals and the d orbital which is singly occupied in the $d^9s$ configuration at the dissociation limit. This active space was used at the minimum. Around the saddle point, however, it led to severe convergence problems and after some experimenting it was found that if the antisymmetric combination of the bonds was excluded from the active space, good convergence was again obtained. Removing one of the bonding orbitals from the active space in a bond-breaking process might seem like a dangerous thing to do. It was, however, checked that this procedure led to reasonable orbitals for the CI calculations. The CASSCF results, on the other hand, will, of course, not be very accurate and are therefore not discussed further. The number of configurations in the CASSCF calculations varies between 12 and 152.

In the contracted CI calculation,[12] 12 electrons were correlated: the Ni–C bonding electrons in the $Ni(CH_3)_2$ reaction and the Ni–H and Ni–C bonding electrons in $Ni(H)CH_3$, respectively, plus the remaining 3d electrons on nickel. Outside the transition state some of these electrons are clearly in other types of orbitals, such as C–C (or one C–H bond in $CH_4$) and nickel 4s orbitals, and are still correlated. Configurations with coefficients larger than 0.07 in a valence CI calculation were used as reference states in the single and double excitation CI. Different CI expansions are used for different parts of the surface; i.e., one expansion is used for the determination of the bent minimum, one for the saddle point, and so on. The number of configurations in the CI calculations varied between 30 000 and 130 000 for $Ni(CH_3)_2$ and between 20 000 and 55 000 for $Ni(H)CH_3$ depending on the part of the potential surface. All CI energies include Davidson's correction[20] as an estimate of the contributions from higher excitations. One problem in the CI calculations was that, except for the linear and dissociated systems, the inactive $CH_3$ bonding orbitals became mixed with the inactive d orbitals in the SCF and CASSCF calculations. Since the C–H bonding electrons were not correlated, the orbitals had to be localized before they were used in the CI calculation. This localization was done in the simplest possible way, performing a unitary rotation between the orbitals pairwise, maximizing the d contribution in one of them. If more than two orbitals per symmetry were involved, an iterative scheme was used. Localization of orbitals was not performed in the determination of the bent minimum and the $^3B_1$ saddle point for $Ni(CH_3)_2$. In a test calculation using the SCF orbitals for the bent minimum of $Ni(CH_3)_2$, the localization of the C–H bonds and the d orbitals lowered the energy by 4 kcal/mol. A reoptimization of these two stationary points using localized orbitals might therefore change the geometries, but it is not probable that the energies will change by more than 1 or 2 kcal/mol.

For the determination of the saddle point for the $^3B_1$ state, the same procedure as for $NiH_2$ was used.[3] Two sets of orbitals are obtained as combinations of orbitals from SCF calculations on the two configurations dominating the wave function on each side of the saddle point. CI calculations were performed for both sets of orbitals and the lowest value was taken to describe the ground-state potential surface.

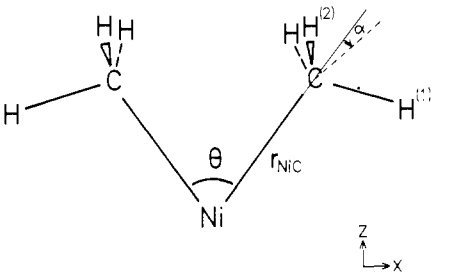


**Figure 1.** Definitions of geometric parameters and position of the coordinate system.

The coordinate systems used for the two molecules are shown in Figure 1, together with the definitions of the different angles and distances. The eclipsed form of ethane was used, which makes the reaction take place in $C_{2v}$ symmetry for $Ni(CH_3)_2$. At the bent minimum the energy difference for the rotation of one methyl group was calculated to be around 1 kcal/mol, with the $C_{2v}$ geometry lowest. For the $Ni(H)CH_3$ reaction the calculations were performed in $C_s$ symmetry.

## 3. Results

The main objective of this study is to compare the reductive elimination and oxidative addition reactions (eq 1) for the three types of bonds: H–H, C–C, and C–H. The basic mechanisms of reaction 1 were elucidated previously in the study of $NiH_2$,[3] and the most important results from that study will therefore be recalled here. Several states of $NiH_2$ were investigated. For a linear geometry the triplet states are lower than the singlet states, with the $^3\Delta_g$ as the ground state. For a bent geometry, however, the $^1A_1$ state is much lower in energy than the rest of the states and was found to have a minimum 8 kcal/mol below the dissociation limit, $Ni(^1D)$ plus $H_2$. The barrier for the addition reaction is very low, only 3 kcal/mol, which can be explained by the fact that the Ni–H bonds start to form simultaneously as the H–H bond breaks and most of the energy lost in the bond-breaking process is regained in the formation of the new bonds. It is the spherical symmetry of the hydrogen atoms that allows them to bind to nickel and the other hydrogen atom at the same time, and it may therefore be expected that the replacement of hydrogen with methyl groups should increase the reaction barrier, since the methyl groups cannot as easily form bonds in several directions. The present calculations confirm this prediction, yielding an addition activation energy of 42 kcal/mol for breaking the C–C bond in ethane and 54 kcal/mol for breaking one of the C–H bonds in methane. See Figure 2 and Tables I and II.

The difference between the hydrogen atoms and the methyl groups also affects the geometry of the bent equilibrium. For all three molecules the bonds are formed from sd hybrids on nickel,

(20) E. R. Davidson in "The World of Quantum Chemistry", R. Daudel and B. Pullman, Eds., Reidel, Dordrecht, 1974.

Table III. $Ni(CH_3)_2$ ($^3B_1$): Geometries[a] and Energies[b]

| geometry | R(Ni-C) | R(C-C) | θ | α | R(Ni-CC) | rel energy |
|---|---|---|---|---|---|---|
| asymptote ($Ni(^3F) + C_2H_6$) | | 2.92 | | | 15.0 | 0 |
| transition state | 4.0 | 4.3 | 65 | 25 | 3.4 | 64.4 |
| linear equilibrium | 3.9[c] | 7.8[c] | 180 | 0 | 0 | 8.0 |

[a] Distances in au and angles in deg. For definition of the angles see Figure 1. [b] Energies in kcal/mol. [c] Only one point computed. R(Ni-C) is taken from the $^1A_1$ state. (Compare $NiH_2$[3] where the two states have similar bond distances.)

Table IV. $Ni(CH_3)_2$ ($^1A_1$): Mulliken Population Analysis (Gross)

| | Ni | | | C | | | |
|---|---|---|---|---|---|---|---|
| | 3d | 4s | 4p | 2s | 2p | $H^{(1)}$ 1s | $H^{(2)}$ 1s |
| asymptote ($Ni(^1D) + C_2H_6$) | 8.99 | 1.00 | 0.01 | 1.27 | 3.10 | 0.88 | 0.88 |
| transition state | 8.88 | 0.97 | 0.27 | 1.33 | 3.15 | 0.78 | 0.83 |
| bent equilibrium | 8.78 | 0.80 | 0.24 | 1.34 | 3.17 | 0.87 | 0.86 |
| linear equilibrium | 8.39 | 0.63 | 0.56 | 1.30 | 3.29 | 0.88 | 0.88 |

Table V. $Ni(H)CH_3$ ($^1A'$): Mulliken Population Analysis (Gross)

| | Ni | | | C | | $H^{(act)}$ | | | |
|---|---|---|---|---|---|---|---|---|---|
| | 3d | 4s | 4p | 2s | 2p | 1s | 2p | $H^{(1)}$ 1s | $H^{(2)}$ 1s |
| asymptote ($Ni(^1D) + CH_4$) | 8.99 | 1.00 | 0.01 | 3.29 | 3.09 | 0.93 | 0.03 | 0.89 | 0.89 |
| transition state | 8.72 | 1.13 | 0.20 | 3.35 | 3.17 | 0.90 | 0.03 | 0.82 | 0.84 |
| equilibrium | 8.75 | 0.85 | 0.19 | 3.34 | 3.19 | 1.07 | 0.01 | 0.88 | 0.85 |

which would give an optimal R–Ni–R angle close to 90°. For $NiH_2$ this angle is only 50°, which shows that there is still an appreciable amount of H–H bonding left. For both $Ni(CH_3)_2$ and $Ni(H)CH_3$ this angle is much closer to 90°, 94° for both of them, which shows that there is no C–C or C–H bonding influencing the equilibrium geometry. This difference in the bonding at the bent equilibrium can also be seen on the binding energies where $NiH_2$ has a larger binding energy, 8 kcal/mol, than $Ni(CH_3)_2$ and $Ni(H)CH_3$, which both have negative binding energies, −5 and −21 kcal/mol, respectively.

The present results can be compared with other theoretical investigations. Using extended Hückel calculations, Tatsumi et al.[16] studied reductive elimination of ethane from $(PH_3)_2Ni(CH_3)_2$. For the elimination reaction these authors obtained a barrier of about 15 kcal/mol, substantially lower than our values of 37 kcal/mol. On the other hand, their activation energy for the addition reaction is approximately 55 kcal/mol compared with our value of 42. The main difference between the two results can be described as a destabilization of the minimum compared to the dissociation limit in their calculation, the minimum being around 40 kcal/mol above the dissociated system, compared with 5 kcal/mol in our case. The difference in the results obtained in the two calculations is probably caused both by the fact that we have no additional ligands on nickel and that we have included correlation effects. The importance of correlation can be seen on our results for $NiH(CH_3)$, where the binding energy at the SCF level is −40 kcal/mol, but only −21 kcal/mol at the CI level. The geometry of the transition state obtained by Tatsumi et al. is fairly similar to the one calculated in the present work.

Balazs et al.[6] performed Xα calculations on $(PH_3)_2NiR_1R_2$ complexes, where $R_1$ and $R_2$ are hydrogen atoms or methyl groups. They calculated the wave function in one single point and used geometries extrapolated from similar experimental structures. They then tried to correlate the observed trends in reaction rates for the reductive eliminations with the characteristics of the local electronic structure of the reactants. Since they do not compute total energies or geometries, their results are difficult to compare with ours. However, they propose the possibility of a triangular bond in $NiH_2$ and that this kind of bond cannot be formed when methyl groups replace the hydrogens. This difference between hydrogen atoms and methyl groups has thus been confirmed by the present calculations.

The results from our calculations are summarized in Tables I–V and Figures 2 and 3. Tables I–III contain reaction energies and geometries for the different states and molecules and Tables IV and V contain Mulliken gross atomic populations for the

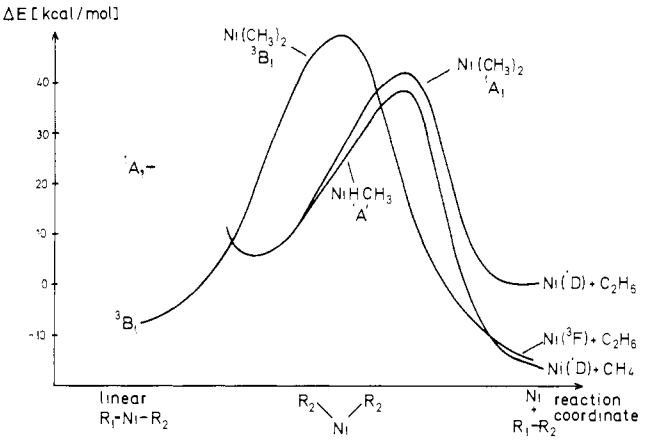


**Figure 2.** Dissociation curves for the $^1A_1$ and $^3B_1$ states of $Ni(CH_3)_2$ and the $^1A'$ state of $Ni(H)CH_3$. The dissociated $Ni(^1D)$ plus ethane is set to zero for dimethylnickel. To simplify the comparison between dimethylnickel and hydromethylnickel for the elimination reaction, the zero point of hydromethylnickel is chosen to put the bent equilibria for the two molecules at the same position.

$^1A_1/^1A'$ states. The relative reaction energies for all computed states are shown in Figure 2, where the bent minima of dimethylnickel and hydromethylnickel are given the same relative energy to simplify the comparison of the elimination reactions. Figure 3 shows schematic reaction geometries for the $^1A_1/^1A'$ states together with total charges of the atoms and overlap populations of the bonds as computed from Mulliken population analysis. Some details of the results are discussed below.

**a. $^1A_1$ State of $Ni(CH_3)_2$.** The geometry at the bent equilibrium was determined at the SCF level using energy gradients. For the methyl groups a C–H distance of 2.07 au, a H–C–H angle of 112°, and a methyl rocking angle α (see Figure 1) of −11.5° were obtained. This geometry of the methyl groups was then used in a CI optimization of the Ni–C distance and the C–Ni–C angle using SCF orbitals. At the so-obtained equilibrium geometry one CASSCF calculation was performed and the energy in Table I is from a CI calculation using these CASSCF orbitals. Switching from SCF orbitals to CASSCF orbitals lowered the energy by as much as 15 kcal/mol, although many reference states are used also for the SCF orbitals. The determination of the geometry is therefore somewhat uncertain. The large difference comes from the fact that the most important virtual orbital, the Ni–C antibonding orbital of $B_2$ symmetry is very poorly described in the

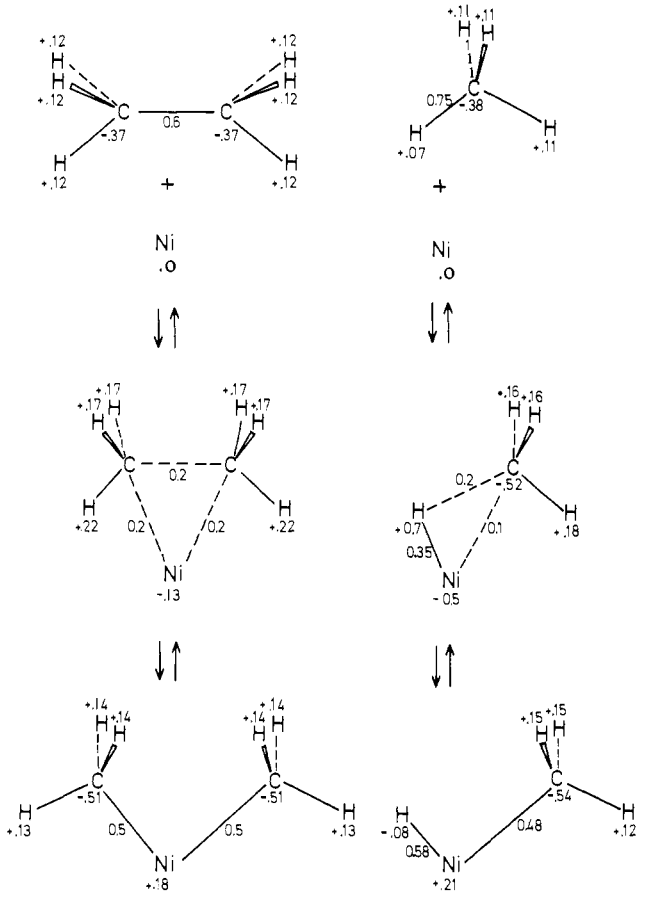

**Figure 3.** Schematic geometries for the stationary points at the reaction surfaces for the $^1A_1/^1A'$ states of dimethylnickel and hydromethylnickel. The total charge on each atom is shown together with total overlap population of each bond.

set of SCF orbitals. The final CI wave function has, however, qualitatively the same appearance for the two sets of orbitals. The saddle point was determined at the CI level varying the Ni–C bond distance, the C–Ni–C angle, and the rocking angle $\alpha$. In this case CASSCF orbitals were used as one particle basis, and the internal geometry of the methyl groups was taken from the minimum, since it is very similar to the ethane geometry. At the dissociation limit one single calculation was performed using the experimental geometry of ethane and with nickel in the $^1D(d^9s)$ state. A linear geometry is also determined from CASSCF and CI calculations. From the similarities with $NiH_2$ an inner saddle point is also predicted but has not been determined in this investigation.

The geometries obtained at the different stationary points are listed in Table I. The Ni–C distances are not very different, 3.89 au for the linear geometry, 3.93 au for the bent minimum, and 4.03 au for the transition state. The C–C distance at the transition state is increased by 1 au compared with that for ethane where it is 2.92 au and at the bent equilibrium it is 5.77 au. The C–Ni–C angle at the transition state is 58° and the rocking angle $\alpha$ is 35°. At the bent minimum the C–Ni–C angle is 94.3° and $\alpha$ is −11.5°. The value of $\alpha$ at the minimum is, however, an SCF value, and for $Ni(H)CH_3$ it was shown that a reoptimization at the CI level increased $\alpha$ by 5°. It is therefore probable that the rocking angle for dimethylnickel at the minimum should be closer to zero than the present value indicates. A small negative value is, however, still likely and a rocking angle of 0° is obtained (determined at the CI level) for a C–Ni–C angle of 76°. It is not easy to explain this negative value of $\alpha$ at the minimum, but it can be noticed that the potential surface for small changes in $\alpha$ is very flat. There is no C–C bonding at the bent equilibrium, which can be seen both from the C–Ni–C angle and the fact that there is no total C–C overlap population at this geometry. At the transition state there seems to be some C–C bonding; the overlap population is 0.2 compared with 0.6 in ethane. The Ni–C overlap is 0.2 electron/bond at the transition state, 0.5 at the bent minimum, and 0.7 for the linear geometry.

During reaction 1, nickel is dominated by a $d^9$ configuration. The d population is 8.88 at the transition state and 8.78 at the bent minimum. The total charge on nickel changes from −0.13 at the transition state (and is even more negative just outside the transition state) to +0.18 at the bent minimum. The extra electrons on nickel at large separation are mainly picked up by the $4p_z$ orbital, which is also the most diffuse orbital, pointing toward ethane. This electron transfer is not likely to be a basis set superposition effect, since the energy has increased. At the transition state the 4s orbital has 0.97 electron and the 4p orbital 0.27 electron, and at the bent minimum these numbers have changed to 0.80 and 0.24, respectively, with the 4p electrons now residing in both the $p_x$ and $p_z$ components. It could therefore be appropriate to describe the bonding as spd hybridization on nickel at the bent minimum. In ethane the total charge on carbon is −0.37 (in the present calculation) and on hydrogen consequently +0.12. At the transition state the charge on the carbons has increased to −0.49. Each of the four out-of-plane hydrogens has the charge +0.17 and the two in-plane hydrogens +0.22. At the bent minimum the charge on the carbons is −0.51 and the charges on the different hydrogen atoms are again more equivalent, +0.14 and +0.13, respectively. For the linear geometry the $d^8$ configuration on nickel is more involved, giving a d population of 8.39, a 4s population of 0.63, and a 4p population of 0.56. The total charge is thus +0.43 on nickel, −0.58 on the carbons, and +0.12 on the hydrogens. The electron transfer at both the bent and linear minima is therefore almost exclusively from nickel to carbon. At the transition state, where nickel is negatively charged, the electrons are transfered from the hydrogens, to both nickel and carbon.

The reaction can also be described in terms of molecular orbital changes. At the bent minimum the wave function is dominated by a closed-shell configuration (with coefficient 0.91 in the CI wave function). The $a_1$ combination of the Ni–C bonds involves the 4s orbital on nickel, and the $b_2$ combination involves mainly the $d_{xz}$ orbital on nickel, leaving nickel in a $d^9$ state. There is also a minor nickel 4p involvement in the two bonding orbitals. The second most important configuration is a double excitation from the $b_2$ bonding orbital to the antibonding orbital of the same symmetry. The coefficient for this configuration is 0.25 in the CI wave function, leading to an occupation number of 0.21 in the $b_2$* orbital. In the dissociated system the $a_1$ bonding orbital has transformed to the $\sigma$ bond in ethane, and the $b_2$ bonding orbital is changed into a pure d orbital on nickel. Simultaneously, one of the d orbitals of symmetry $A_1$, which is doubly occupied at the minimum, has become singly occupied, the second electron being promoted into the 4s orbital, again leaving nickel in a $d^9$ state. This last transformation occurs because the $^1D(d^9s)$ state of the nickel atom is 32 kcal/mol lower than the $^1S(d^{10})$ state.[21] The orbitals are smoothly transformed during the reaction, giving orbitals of intermediate character at the transition state. The importance of the excitation into the $b_2$ antibonding orbital decreases during the elimination reaction and the occupation of this orbital is 0.12 at the transition state. The occupation numbers of the nickel $d_{a_1}$ orbital and the weakly occupied orbital of $A_1$ symmetry, which is to become the nickel 4s orbital at the dissociation limit, also vary smoothly, from close to 2.0 and 0.0, respectively, at the minimum to 1.0 and 1.0 at the dissociation limit, continuously compensating for the increased d population in the doubly occupied $b_2$ orbital. In the actual calculations the $d_{a_1}$ and 4s orbital mix to give, e.g., at the transition state one sd hybridized orbital pointing out of the C–Ni–C plane with occupation number 1.6 and another one in the plane with occupation number 0.4.

The linear geometry is 18.5 kcal/mol higher in energy than the bent equilibrium. This result can be compared with the result for the $^1A_1$ state obtained by Åkermark et al.[15] In valence CI calculations they did not obtain any bent minimum for the $^1A_1$

(21) C. E. Moore, "Atomic Energy Levels", U.S. Department of Commerce, National Bureau of Standards, Washington, D.C., 1952.

state, and the energy for a C–Ni–C angle of 90° is 31.6 kcal/mol higher than for the linear geometry. This difference is probably due to the lack of diffuse enough d functions in their basis set which gives an unreasonable splitting between the $d^8$ and $d^9$ states of nickel. With their basis set the $d^9$ configuration becomes far too high in energy to compete with the $d^8$ configuration and they obtain a qualitatively erroneous wave function. The d population at a C–Ni–C angle of 90° is 8.26 in their valence CI wave function, compared with 8.78 in our calculation.

**b. $^1A'$ State of $Ni(H)CH_3$.** The procedure of determining geometries for the stationary points of hydromethylnickel was very much the same as for dimethylnickel. These geometries are listed in Table II. At first the SCF geometry of the equilibrium was determined in five iterations by the gradient program. The internal coordinates of the methyl group were then kept fixed all through the calculations at both the equilibrium and the saddle point. All the remaining four coordinates, the Ni–C and Ni–H bonds, the H–Ni–C angle $\theta$, and the methyl rocking angle $\alpha$, were then varied in CI calculations using CASSCF orbitals to determine the respective geometries of these two points. Correlation did not alter the equilibrium geometry very much. The biggest changes in going from SCF to CI were a lengthening of $R$(Ni–C) from 3.65 to 3.75 au and $\alpha$ changing from −3 to 2°. The energy decrease from changing the geometry was only about 1 kcal. Starting at the obtained minimum the location of the transition state was achieved by choosing $\theta$ as a reaction parameter which was decreased in large steps while minimization of the other three coordinates were performed in CASSCF calculations. When the transition state area was reached the determination of the saddle point was made in CI calculations. In the beginning of the reaction only $\theta$ varies, while there is a strong coupling between $\theta$ and $\alpha$ in the transition state region. At the transition state $\theta$ is 50° and $\alpha$ has increased to 25°. The Ni–C bond has been considerably lengthened from 3.74 to 4.0 au, whereas $R$(Ni–H) is constant at about 2.80 au. Finally one calculation at the dissociation limit was performed with $CH_4$ in the experimental geometry.

The course of addition of methane to nickel is similar to that of ethane, but some new features are introduced. Because of the lower symmetry of the system, the orientation of the approaching $CH_4$ is not clear. The geometry of the transition state suggests that the active hydrogen starts to bind to nickel before carbon does, and this is confirmed by the overlap populations. At the transiton state the Ni–C overlap is only 0.10 compared with 0.48 in the composite system. Corresponding figures for Ni–H are 0.35 and 0.58, respectively. The C–H bond at the transition state is broken to the same extent as the C–C in the addition of ethane; the overlap has decreased from 0.75 in methane to 0.20.

Charge transfers are similar to those of the ethane addition. Nickel gets initially slightly negatively charged but ends up with a charge of +0.21 at the equilibrium. The d population on nickel is about 8.7 and stays nearly constant throughout the reaction with charge fluctuations mainly taking place in the diffuse part of the 4s orbital. The methyl group is polarized into a negative carbon and positive hydrogens, and this polarization is strongest around the transition state. The active hydrogen is slightly positive both in methane and at the transition state, but then picks up charge from nickel and ends up slightly negative.

The description of the reactions of methane and nickel in terms of molecular orbital changes and dominating configurations is very similar to that of the ethane reactions given above. In this case, however, one of the carbons in the nickel–ethane reactions has been replaced by a hydrogen atom and all the bonding and antibonding orbitals are of A′ symmetry. One of the nickel–methane bonding orbitals involves the 4s orbital on nickel and behaves similarly to the $a_1$ bonding orbital in the nickel–ethane system. The other nickel–methane bonding orbital involves the nickel $d_{xz}$ orbital and plays the role of the $b_2$ bonding orbital in nickel–ethane.

**c. $^3B_1$ State of $Ni(CH_3)_2$.** The triplet states of $NiH_2$ have only linear minima.[3] The $^3B_1$ state, which is the ground state ($^3\Delta_g$ in linear symmetry), was found to have the lowest barrier of all the triplet states for the elimination reaction, 42 kcal/mol. The H–Ni–H angle at the transition state was 56° and the linear geometry had almost the same energy as the dissociation limit (Ni($^3$F) plus $H_2$). To compare the behavior of the triplet states of $NiH_2$ and $Ni(CH_3)_2$, the potential surface of the $^3B_1$ state of $Ni(CH_3)_2$ was also calculated. The barrier for the elimination reaction is somewhat higher for $Ni(CH_3)_2$, around 56 kcal/mol compared with 42 kcal/mol for $NiH_2$, and the linear equilibrium geometry is 8 kcal/mol above the dissociation limit. The C–Ni–C angle, around 65°, is somewhat larger than for $NiH_2$ and the rocking angle $\alpha$ is around 25°. The wave function has the same characteristic behavior as for $NiH_2$, changing suddenly from one dominating configuration at one side of the saddle point to another one at the other side of the saddle point. The internal geometry of the methyl groups for this state was taken from ref 15.

## 4. Conclusions

The most important result of the present investigation is that the expected differences between the hydrogen molecule on one side and methane and ethane on the other side, during an oxidative addition reaction have been confirmed. The computed barriers for breaking a C–H or a C–C bond are considerably higher than for the H–H bond, 54 and 42 kcal/mol respectively, compared with 3 kcal/mol for $H_2$, and this is in agreement with experiment. This difference has been attributed to the difference between the hydrogen atom and the methyl group in the ability to form bonds in several directions at the same time. The C–C bond in ethane has to break almost completely before the Ni–C bonds can start to form, which is not the case for the H–H bond in the formation of $NiH_2$. The barrier for addition of methane could have been expected to lie somewhere between the hydrogen and ethane values, since then one of the R groups has the mentioned flexibility. But this does not turn out to be the case. Instead, the barrier for methane is somewhat higher than for ethane, which can be explained by the fact that the C–H bond in methane is stronger than the C–C bond in ethane, 104 and 88 kcal/mol, respectively.[22] This difference at the dissociation limit also explains the difference in binding energy at the equilibrium geometry, since the Ni–H and the Ni–C bonds are expected to be of approximately the same strength, computed by Goddard et al.[23] to be 64 and 60 kcal/mol, respectively. We found the nickel–ethane binding energy to be 15.4 kcal/mol larger than for nickel and methane.

Looking at the reaction in the other direction, the reductive elimination reaction, the barriers for $Ni(CH_3)_2$ and $Ni(H)CH_3$ are very similar, 37 and 33 kcal/mol, respectively, which should be compared with an activation energy of 11 kcal/mol for $NiH_2$. It has been suggested that the near-total absence of stable transition metal alkyl hydrides together with the large number of known stable dialkyls and dihydrides, could imply that the elimination of alkyl hydride is a faster reaction than the elimination of hydrogen or alkyl–alkyl.[7] Our calculations do not indicate such an order of the reaction rates, and the high barrier for the methane elimination is not consistent with the absence of observed alkyl hydrides. Addition of destabilizing ligands can, however, lower the barriers considerably, and the small difference between methane and ethane in barrier height might then become important. It should also be noted, as pointed out in sections 2 and 3, that the determination of the minimum for dimethylnickel is somewhat less accurate than for the rest of the stationary points, and a lowering of the equilibrium energy for dimethylnickel will increase the difference in barrier heights between dimethylnickel and hydromethylnickel. Another interesting feature, that should be noted in Figure 2, is that for $Ni(CH_3)_2$ the barrier height of the $^1A_1$ state and the $^3B_1$ state are very similar. This is a difference compared with $NiH_2$, where the triplet states were much higher than the $^1A_1$ state. Thus, the triplet states of nickel complexes also can be of interest for these kinds of reactions.

A few comments should be made about the accuracy of the obtained results. Because of the complexity of the systems studied,

(22) J. A. Kerr and A. F. Trotman-Dickenson in "Handbook of Chemistry and Physics", R. C. West., Ed., The Chemical Rubber Co., Cleveland, Ohio, 1968, p F-163.

(23) W. A. Goddard III, S. P. Walch, A. K. Rappe, T. H. Upton, and C. F. Melius, *J. Vac. Sci. Technol.*, **14**, 416 (1977).

it is not possible to obtain a very high quantitative accuracy. The intention of the present work is to get qualitatively correct results, and energy differences of a few kilocalories should not be interpreted as significant differences. The most severe limitation of the calculations when the results are compared with experimental observations is, of course, the model systems used, the fact that there are no extra ligands on nickel, that there is no solution around the complex, and so on. But within the present model the most severe restriction is probably the quality of the basis set. Test calculations did, however, show that neither f functions on nickel nor d functions on carbon change the results qualitatively. The main effect of f functions on nickel is to give a better energy splitting of the atomic states, and since the d population on nickel is fairly constant along the potential surface, the f functions are not expected to influence the shape of the surface very much. d functions on carbon decreased the binding energy of $Ni(CH_3)_2$ by 4 kcal/mol, from −5 to −9 kcal/mol.

**Acknowledgment.** We are grateful to docent Björn Åkermark for many helpful and stimulating discussions about the experimental results for reductive elimination and oxidative addition reactions. We also thank the institute of Inorganic Chemistry at the University of Zürick for the hospitality during parts of these calculations and especially Hans Peter Lüthi for valuable help. This work has been supported by a grant from the Swedish Research Council (NFR).

**Registry No.** $Ni(CH_3)_2$, 54836-89-4; $Ni(H)CH_3$, 86392-32-7; Ni, 7440-02-0; ethane, 74-84-0; methane, 74-82-8.

# Ionization Potentials, Electron Affinities, and Molecular Orbitals of 2-Substituted Norbornadienes. Theory of 1,2 and Homo-1,4 Carbene Cycloaddition Selectivities

**K. N. Houk,*[1a,c,d] Nelson G. Rondan,[1c,d] Michael N. Paddon-Row,[1b–d] Charles W. Jefford,*[1e] Phan Thanh Huy,[1e] Paul D. Burrow,[1f] and K. D. Jordan[1c]**

*Contribution from the Departments of Chemistry, University of Pittsburgh, Pittsburgh, Pennsylvania 15260, Louisiana State University, Baton Rouge, Louisiana 70803, and University of Geneva, 1211 Geneva 4, Switzerland, and the Department of Physics, University of Nebraska, Lincoln, Nebraska 68588.* *Received February 28, 1983*

**Abstract:** The ionization potentials, electron affinities, and $\pi$ orbital shapes of 2-substituted norbornadienes have been determined by photoelectron spectroscopy, electron-transmission spectroscopy, and ab initio molecular orbital calculations, respectively. The deductions made about the electronic structures of 2-methoxy-, (trimethylsiloxy)-, chloro-, cyano-, (methoxycarbonyl)-, and phenylnorbornadienes permit a detailed interpretation of the reactivities and selectivities observed experimentally in carbene cycloadditions to these molecules. A substituent at C-2 of norbornadiene not only affects the 2–3 $\pi$ bond but also influences the 5–6 $\pi$ bond due to through-space interactions between $\pi$ orbitals. The orbital energy changes and polarization induced by 2-substituents provide a compelling rationale of the variations in 1,2 and homo-1,4 cycloadditions of carbenes to these species, and confirm the electrophilic nature of both of these cycloadditions.

Can anything more be discovered about subtle electronic effects in norbornadiene? This molecule and derivatives thereof have been subjected to virtually every type of chemical abuse imaginable, yet new phenomena continue to pour forth from experimental and theoretical studies of this battered framework. Apart from the monumental accumulation of data on the solvolysis of norbornyl derivatives, the amount of information about electrophilic,[2] nucleophilic,[3] and radical reactions[4] on norbornenes and norbornadienes is substantial. Our own interests in norbornadienes have been in the study of Diels–Alder,[5] carbene,[6,7] and singlet-oxygen[8] reactions of these molecules, as well as our studies of the molecular deformations of the alkene moieties caused by the basic ring skeleton together with its substituents.[9]

Our new obsession with 2-substituted norbornadienes arose from the discovery in the Geneva laboratories of the exo-1,2, endo-1,2, and endo-homo-1,4-cycloadditions defined in Figure 1. In 2-

**Table I.** Adducts Obtained from the Addition of Difluorocarbene to 2-Substituted Norbornadienes[a]

| reactant 2-R-norbornadiene R = | exo-1,2 adducts | | endo-homo-1,4 adducts | | exo-1,2/ homo-1,4 ratio |
|---|---|---|---|---|---|
| | syn | anti | anti | syn | |
| -OMe | 89.0 | | 11.0 | | 8.1 |
| $-OSiMe_3$ | 75.0 | 6.0 | 6.0 | | 4.2[b] |
| -Ph | 75.0 | | 25.0 | | 3.0 |
| -Cl | 62.0 | 4.0 | 34.0 | | 1.9 |
| -H | 33.0 | 33.0 | 34.0 | | 1.9 |
| $-CO_2Et$ | 44.0 | 12.0 | 44.0 | | 1.3 |
| $-CO_2Me$ | 38.0 | 15.0 | 47.0 | | 1.1 |
| -CN | 35.0 | 23.0 | 30.0 | 12.0 | 1.4 |

[a] Yields are normalized to 100%. [b] Three other products are formed (13%), but have eluded characterization so far. One of these may be the 1,4 adduct.

(1) (a) Address correspondence to this author at the University of Pittsburgh. (b) Permanent address: Department of Chemistry, New South Wales Institute of Technology, N.S.W., Australia. (c) University of Pittsburgh. (d) Louisiana State University. (e) University of Geneva. (f) University of Nebraska.

(2) Freeman, F. *Chem. Rev.* **1975**, *75*, 439. See, for example, Brown, H. C.; Kawakami, J. H.; Liu, K.-T. *J. Am. Chem. Soc.* **1973**, *95*, 2209 and references therein.

(3) See, for example: Richey, H. G., Jr.; Wilkins, C. W., Jr. *J. Org. Chem.* **1980**, *45*, 5027. Richey, H. G., Jr.; Wilkins, C. W., Jr.; Bension, R. M. *J. Org. Chem.* **1980**, *45*, 5042.

(4) See, for example: Davies, D. I.; Parrot, M. J. *Tetrahedron* Lett. **1972**, 2719.

(5) Mazzochi, P.; Stahly, B.; Dodd, J.; Rondan, N. G.; Domelsmith, L. N.; Rozeboom, M. D.; Caramella, P.; Houk, K. N. *J. Am. Chem. Soc.* **1980**, *102*, 6482.

(6) Jefford, C. W.; Kabengele, nT.; Kovacs, J.; Burger, U. *Helv. Chim. Acta* **1974**, *57*, 104; *Tetrahedron Lett.* **1974**, 257; Kwantes, P. M.; Klumpp, G. W. *Ibid.* **1976**, *707*. Jefford, C. W.; Mareda, J.; Gehret, J. C. E.; Kabengele, nT.; Graham, W. D.; Burger, U. *J. Am. Chem. Soc.* **1976**, *98*, 2585.

(7) Jefford, C. W.; Phan Thanh, Huy *Tetrahedron Lett.* **1980**, 755.

(8) Jefford, C. W.; Rimbault, C. G. *J. Org. Chem.* **1978**, *43*, 1908; *J. Am. Chem. Soc.* **1978**, *100*, 295, 6437, 6515; *Tetrahedron Lett.*, **1979**, 985.

(9) Rondan, N. G.; Paddon-Row, M. N.; Caramella, P.; Houk, K. N. *J. Am. Chem. Soc.*, **1981**, *103*, 2438.

0002-7863/83/1505-5563$01.50/0 